

A Z_2 spin-orbital liquid state in the square lattice Kugel-Khomskii model

Fa Wang^{1,2} and Ashvin Vishwanath^{1,2}

¹*Department of Physics, University of California, Berkeley, CA 94720*

²*Materials Sciences Division, Lawrence Berkeley National Laboratory, Berkeley, CA 94720*

(Dated: Printed October 30, 2018)

We argue for the existence of a liquid ground state in a class of square lattice models of orbitally degenerate insulators. Starting with the SU(4) symmetric Kugel-Khomskii model, we utilize a Majorana Fermion representation of spin-orbital operators to access novel phases. Variational wave functions of candidate liquid phases are thus obtained, whose properties are evaluated using variational Monte Carlo. These states are disordered, and are found to have excellent energetics and ground state overlap ($> 40\%$) when compared with exact diagonalization on 16 site clusters. We conclude that these are spin-orbital liquid ground states with emergent nodal fermions and Z_2 gauge fields. Connections to spin 3/2 cold atom systems and properties in the absence of SU(4) symmetry are briefly discussed.

I. INTRODUCTION

In correlated insulators, the degrees of freedom that remain at low energies are spin and orbital degeneracy. At low temperatures one usually obtains an ordered state described essentially by a classical variable, the Landau order parameter. Ground states that are not described by the Landau framework are expected to possess strikingly new properties. While they are known to occur in one dimensional systems, an important question is whether they arise in bulk two and three dimensional materials. Theoretical studies have largely focused on quantum spin systems. While model Hamiltonians for spin liquids exist, one needs special conditions like strong frustration to ensure that the spins do not order. Otherwise, even for spin 1/2 quantum fluctuations are not typically strong enough to destroy order. On the other hand, orbital degeneracy in insulators can enhance quantum fluctuations,^{1,2,3} destroying order and possibly lead to a spin-orbital liquid state. An experimental illustration is provided by the insulating spinels $MnSc_2S_4$ and $FeSc_2S_4$. The former, a pure $S=5/2$ system, magnetically orders below 2Kelvin. The latter, a spin $S=2$ system, is identical in most respects except that it involves a twofold orbital degeneracy. In contrast to the spin system, it is found to remain spin disordered down to the lowest temperatures of 30mKelvin.⁴

Here, we theoretically study a simple spin 1/2 square lattice model with the minimal twofold orbital degeneracy. Such a spin-orbital Hilbert space is realized for e.g. with the $d_{3z^2-r^2}$, $d_{x^2-y^2}$ orbitals of Ag^{2+} , Cu^{2+} or (low spin) Ni^{3+} in an octahedral environment. We focus on a model that captures the effect of enhanced quantum fluctuations from orbital degeneracy, and argue for a liquid ground state in this case. We give theoretical arguments for the stability of this phase as well as well as a numerical Monte Carlo study of a variational wave function. The latter is found to have extremely good energetics for our Hamiltonian, and allows us to characterize this phase beyond the simple fact that it is disordered. The low energy collective excitations of the liquid state

are captured by an emergent Z_2 gauge field, coupled to Dirac like fermionic excitations with fractional spin and orbital quantum numbers. The ground state wavefunction is strongly entangled, and can be thought of as a product of three Slater determinant wave-functions.

Realistic spin-orbital Hamiltonians tend to be rather complicated with several exchange couplings that are strongly direction dependent. Moreover, a linear coupling between the orbital degrees of freedom and the Jahn-Teller phonons can quench coherent orbital dynamics. However, for sufficiently strong exchange interactions, the coupling to phonons can be ignored, and the orbitals can be taken to be quantum degrees of freedom. Since we are interested here in the general effects of enhanced quantum fluctuations from orbital degeneracy, we follow³ and others in considering a model that treats all four states on a site symmetrically, i.e. the SU(4) symmetric spin orbital model. This will allow for comparisons and is a useful starting point. We show later that our essential conclusions are unchanged on perturbing away from this high symmetry point.

The high symmetry SU(4) model may, in fact, have a direct physical realization. We point out that a model of e_g orbitals on certain high symmetry lattices, like the diamond lattice, can have spin orbital Hamiltonian that are nearly SU(4) symmetric. A different setting for this physics has been opened up by the recent experimental developments on the trapping and cooling of alkaline earth atoms. Confining these to the sites of an optical lattice leads to SU(N) symmetric magnetic models. The nuclear spin here provides the N flavors, and, given the weak dependence of scattering lengths on nuclear spin, leads to SU(N) symmetric exchange interactions, which, for fermionic atoms, will be antiferromagnetic.⁵ Fermionic alkaline-earth like atoms of ^{173}Yb have been cooled to quantum degeneracy,⁶ while the Mott state of the bosonic ^{174}Yb has been recently realized.⁷ A different realization may be provided by spin 3/2 cold atoms, such as ^{132}Cs confined to the sites of an optical lattice. At unit filling, one has four states per site, and although the physical symmetry is only that of spin rotations, the small difference in scattering lengths imply only a weak

breaking of SU(4) symmetry. It was pointed out in⁸ that even including these differences only breaks the symmetry down to SO(5) \times Z₂ in the low energy limit.

II. THE MODEL:

We study the SU(4) symmetric Kugel-Khomskii model^{9,10} on the *square lattice*:

$$H = \frac{J}{4} \sum_{\langle ij \rangle} (\vec{s}_i \cdot \vec{s}_j + 1)(\vec{\tau}_i \cdot \vec{\tau}_j + 1) \quad (1)$$

where \vec{s} are the spin-1/2 Pauli matrices and $\vec{\tau}$ are the Pauli matrices acting on the two degenerate orbital states. We consider the antiferromagnetic (AFM) case ($J > 0$) and set $J = 1$ hereafter. The high symmetry of this model implies that the three spin operators \vec{s} , three orbital operators $\vec{\tau}$ and nine spin orbital operators $\sigma^a \tau^b$ all appear with equal weight. These are fifteen generators of SU(4). It should be noted that symmetry does not uniquely define a model, one also needs to specify the representation of the symmetry group appearing at each site. Here the fundamental representation appears and an SU(4) singlet can only be formed between four sites.

The model (1) was numerically studied in³ using exact diagonalization (the model suffers from a sign problem in the spin-orbital basis) on system sizes of up to 4×4 . The ground state ($E = -17.4$) is an SU(4) singlet at zero wavevector. Simple trial states, such as with spin-orbital order, or a box singlet state, have much higher average energy ($E = 0$ and $E = -12$ respectively) pointing to the importance of quantum fluctuations. This motivates the study of spin orbital liquids as candidate ground states.

The idea of resonating valence bonds,^{11,12} provides an intuitive picture of the quantum spin liquid. A more formal approach that is easier to generalize is the slave particle formalism, where the spin is decomposed into 'partons', e.g. $\vec{s}_r = \sum_{\sigma, \sigma'} a_{\sigma r}^\dagger \vec{\sigma} a_{\sigma' r}$, where the $\vec{\sigma}$ are the Pauli matrices, and $(a_{\uparrow r}^\dagger, a_{\downarrow r}^\dagger)$ creates a boson (Schwinger boson) or fermion with spin (\uparrow, \downarrow) at site r , and the constraint $\sum_{\sigma} a_{\sigma r}^\dagger a_{\sigma r} = 1$ is imposed at every site. One then makes a mean field decomposition to obtain a quadratic Hamiltonian, and the constraint is then imposed by projecting the wave function to obtain a variational ground state. The state so obtained is a candidate spin-liquid wave function. This procedure can be generalized in a straightforward way to the spin-orbital Hilbert space at hand, by introducing a four component a_σ and the constraint above at every site.^{13,14} The physical spin and orbital operators are again bilinears of a_σ . However, there are some drawbacks to this straightforward generalization. The bosonic parton representation cannot treat the SU(4) symmetric point, while the fermionic parton theories necessarily lead to Fermi surface states which can be hard to stabilize as ground states.

Below, we will sidestep these difficulties by showing that this problem admits a third, physically distinct, parton representation in terms of Majorana Fermions. This representation, which has not previously been applied to two dimensional systems, offers us many advantages. Besides being more economical (in terms of expanding the Hilbert space in the minimal fashion), it leads to liquid states with a Z₂ gauge group, whose low energy physics is well understood and known to exist as stable phases. We emphasize here that the projected wavefunction obtained from this Majorana parton representation of the SU(4) model is distinct from the 'Schwinger' fermion representation, involving four fermionic a_σ operators.

III. MAJORANA PARTON FORMULATION:

We first point out the group isomorphism SU(4) \equiv SO(6). The 15 generators of the latter are dimension six antisymmetric real matrices $L_{\mu\nu}^A$, where $A = 1 \dots 15$ and $\mu, \nu = 1 \dots 6$. An operator representation of this algebra is obtained by introducing six Majorana fermions (χ_1, \dots, χ_6) which satisfy the anticommutation relations $\{\chi_\mu, \chi_\nu\} = 2\delta_{\mu\nu}$. The operators $\hat{O}^A = \frac{1}{4} L_{\mu\nu}^A \chi_\mu \chi_\nu$, where summation over repeated indices is assumed, reproduce the commutation relations for SO(6) generators. The Majorana Fermions transform as SO(6) vectors.

We now use the group isomorphism to obtain a representation of the spin-orbital operators, in terms of Majorana fermions. It is helpful to write the set of Majorana fermions as a pair of three component vectors $(\vec{\theta}_r, \vec{\eta}_r)$ where, e.g. $\vec{\theta}_r = (\theta_{1r}, \theta_{2r}, \theta_{3r})$ and we have introduced site indices r . The spin and orbital operators can then be written in the compact form:

$$\vec{s}_r = -\frac{i}{2} \vec{\eta}_r \times \vec{\eta}_r, \quad \vec{\tau}_r = -\frac{i}{2} \vec{\theta}_r \times \vec{\theta}_r \quad (2)$$

and $s_r^\mu \tau_r^\nu = -i \eta_{\mu r} \theta_{\nu r}$, which automatically obey the expected algebra. Note, the sign of the Majorana fermion operators can be changed without affecting the physical operators. This Z₂ redundancy is connected to the fact that the Hilbert space is now enlarged - since each Majorana fermion corresponds to $\sqrt{2}$ degrees of freedom, we have $(\sqrt{2})^6 = 8$ states whereas there are only 4 physical states per site. The excess states can be removed by implementing a Z₂ constraint at each site: first define the operator ν_r commutes with the physical operators (which are fermion bilinears) and is idempotent $\nu_r^2 = 1$.

$$\begin{aligned} \nu_r &\equiv i \theta_{1r} \theta_{2r} \theta_{3r} \eta_{1r} \eta_{2r} \eta_{3r} \\ \nu_r &= 1, \quad \forall r \end{aligned} \quad (3)$$

Hence implementing the constraint in (3), restricts us to the physical Hilbert space. This operator generates the Z₂ gauge transformation on the Majorana fermions $\theta_{\alpha r} \rightarrow -\theta_{\alpha r}, \eta_{\alpha r} \rightarrow -\eta_{\alpha r}$.

The model in (1) can be written in these variables as:

$$H = \sum_{\langle jk \rangle} \left[1 - (1/8) \left(i\vec{\eta}_j \cdot \vec{\eta}_k + i\vec{\theta}_j \cdot \vec{\theta}_k \right)^2 \right] \quad (4)$$

When supplemented by the constraint (3), this is an exact rewriting of the model. Here, the $SO(6)$ symmetry of the model is explicit. The quartic nature of the Hamiltonian requires an approximation. We begin with a mean field treatment and use it to generate variational states in which the constraint is treated exactly.

In the context of models with only spin 1/2 (and no orbital degrees of freedom) we note that a representation utilizing three Majorana fermions per site, where the spin operator \vec{s}_r is given by an expression identical to that in Eqn. 2, has been studied.¹⁵ However, we point out that this is distinct from our current formalism since a single site constraint cannot be applied to generate the physical Hilbert space. Nevertheless, this provides an alternate parton approach - for example, with an even number of sites, one can view half of the spins as ‘orbital pseudo-spins’, then the spin problem will be artificially converted to a spin-orbital problem, (although without $SU(4)$ symmetry). Then the gauge fixing, and construction of complex fermions and variational wave functions can be proceeded in the same fashion as in this paper. But this artificial discrimination of spin and ‘orbital pseudo-spin’ usually will superficially break lattice symmetry. Another way to construct a Hilbert space for the spin 1/2 only model, is to introduce a fourth Majorana fermion on every site, and the set of four fermions satisfies a product constraint as in Eqn. 3.¹⁶ This has the benefit of being formulated with a unique single site constraint. However, unfortunately it turns out that these four fermions are just the real and imaginary parts of the two Schwinger fermion operators, and do not lead to a new representation. The constraint is the familiar one of requiring single occupancy of the Schwinger fermions.

Mean Field Theory and Gutzwiller Projection: With real mean field parameters χ_{jk} ($= -\chi_{kj}$), we have:

$$H_{MF} = \sum_{\langle jk \rangle} \left[1 - (i\chi_{jk}/4) \left(\vec{\eta}_j \cdot \vec{\eta}_k + \vec{\theta}_j \cdot \vec{\theta}_k \right) + \chi_{jk}^2/8 \right] \quad (5)$$

In self consistent mean field theory $\chi_{jk} = i\langle (\vec{\eta}_j \cdot \vec{\eta}_k + \vec{\theta}_j \cdot \vec{\theta}_k) \rangle_{MF}$. For convenience we combine the 6 Majorana fermions into 3 complex fermions: $c_{\alpha r}^\dagger = (1/2)(\eta_{\alpha r} + i\theta_{\alpha r})$ which are more intuitive although the $SO(6)$ symmetry is no longer explicit. The constraint then is: $\sum_{a=1}^3 c_{\alpha r}^\dagger c_{\alpha r} = 0$ OR 2 (while the odd values of the site occupation are forbidden). Writing $\vec{c}_r = (c_{1r}, c_{2r}, c_{3r})$, we have $i(\vec{\eta}_j \cdot \vec{\eta}_k + \vec{\theta}_j \cdot \vec{\theta}_k) = 2i(\vec{c}_j^\dagger \cdot \vec{c}_k - \vec{c}_k^\dagger \cdot \vec{c}_j)$ i.e. the mean field theory simply involves fermions hopping with pure imaginary amplitudes. Such a band structure is automatically particle-hole symmetric, which leads to half-filled bands for each of the c_{ra} fermions. Note, despite the imaginary hoppings the mean field ansatz is time reversal symmetric if the hopping is bipartite. The mean

field wave function is simply a product of three identical Slater determinants. While the specific Slater determinant depends on the mean field ansatz, we make a few general observations below. If we consider a system with $4N$ sites, required to obtain an $SU(4)$ singlet state, each Slater determinant Φ is a function of $2N$ particle coordinates, corresponding to half filling. Gutzwiller projecting the mean field state into the constrained Hilbert space, yields a physical spin-orbital wave-function. In the fermion representation, a site can either have no fermions (denoted by $|0\rangle$), or two fermions, in which case there are three states, $|X\rangle = c_2^\dagger c_3^\dagger |0\rangle$, $|Y\rangle = c_3^\dagger c_1^\dagger |0\rangle$, $|Z\rangle = c_1^\dagger c_2^\dagger |0\rangle$. These are related to the spin orbital basis states via:

$$\begin{aligned} |\sigma^z = \mp 1, \tau^z = \pm 1\rangle &= (|0\rangle \pm i|X\rangle)/\sqrt{2} \\ |\sigma^z = \pm 1, \tau^z = \pm 1\rangle &= (|Y\rangle \pm i|Z\rangle)/\sqrt{2} \end{aligned}$$

Given a configuration specified by the locations of the $|X\rangle$, $|Y\rangle$ and $|Z\rangle$ states (at sites $\{x_i\}$, $\{y_j\}$ and $\{z_m\}$ respectively, where x_i, y_j, z_m are $3N$ distinct positions), the spin-orbital wave function assigns an amplitude $\Psi[\{x_i\}, \{y_j\}, \{z_m\}]$ to it. Note, the locations of the $|0\rangle$ states are automatically specified. For an $SU(4)$ singlet we need equal numbers, N , of the four types of sites, so $\{x_i\} = \{x_1, \dots, x_N\}$ etc. After the Gutzwiller projection we obtain:

$$\begin{aligned} \Psi[\{x_i\}, \{y_j\}, \{z_m\}] \\ = \Phi[\{y_j\}, \{z_m\}] \cdot \Phi[\{z_m\}, \{x_i\}] \cdot \Phi[\{x_i\}, \{y_j\}] \end{aligned} \quad (6)$$

Thus the projected spin-orbital wave function is a product of three Slater determinants with a lot of entanglement. We now apply this formalism to specific models.

IV. ONE DIMENSIONAL CHAIN

This $SU(4)$ symmetric nearest neighbor model in 1D is very well understood and serves as a benchmark for our technique. The only symmetric mean field ansatz is a uniform $\chi_{r,r+1} = \chi$, leading to a dispersion $\epsilon(k) = \chi \sin(k)$. We construct the resulting projected wave function for L site chain with $L = 8, 16 \dots 128$ and antiperiodic boundary conditions, and evaluate its properties using variational Monte Carlo. The energy per site from the projected wave functions extrapolated to the thermodynamic limit is -0.8233 , not far from the exact result,¹⁷ $1 - (1/2) \int_0^1 \frac{x^{-3/4}-1}{1-x} dx = -0.8251$. The leading term in the asymptotic spin correlation function is $\cos(\pi r/2)/r^{1.5}$, consistent with theoretical and numerical predictions.^{18,19,20} Note, these desirable properties of the wavefunction only arise *after* projection. (see TABLE I).

Interestingly, the $\pi/2$ wavevector of the dominant correlations do not correspond to a natural wavevector of the mean field dispersion, and arises entirely from projection. In contrast, this wavevector is easier to understand on projecting a quarter filled band, which arises in the standard fermionic representation of spin-orbital operators

TABLE I: Results of the projected wave function for L -site chain with antiperiodic boundary condition. The second row shows energy per site for the projected wave function. The third row shows the $L^{-1.5}$ scaling of s^z -correlation functions [$s^z(x)$ is s^z at position x].

L	8	16	32	48	64
$\langle H \rangle / L$	-0.8642	-0.8332	-0.8256	-0.8242	-0.8237
$\langle s^z(0)s^z(L/2) \rangle L^{1.5}$	1.66	1.82	1.90	1.92	1.96
L	80	96	112	128	
$\langle H \rangle / L$	-0.8235	-0.8234	-0.8233	-0.8233	
$\langle s^z(0)s^z(L/2) \rangle L^{1.5}$	1.98	1.94	1.97	1.97	

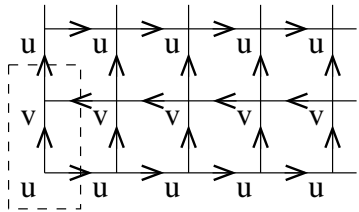


FIG. 1: The π -flux ansatz on the square lattice. An arrow from site j to k means $\chi_{jk} > 0$. Dashed lines enclose the doubled unit cell, with two sites u and v .

a_σ . Remarkably, one can show that the projected wave functions arising from this representation and the Majorana fermion representation discussed above, are *identical in one dimension*. We stress that this is a special feature of one dimension, and in higher dimensions, the two will lead to physically distinct states. Details of the proof can be found in Appendix A.

V. SQUARE LATTICE:

The mean field states on the square lattice can be distinguished by the gauge invariant flux through the elementary plaquettes e.g. $\chi_{jk}\chi_{kl}\chi_{lm}\chi_{mj}$ for the plaquette $jk\ell m$. Translation and Time reversal symmetry dictates that this flux must be uniform and can be either 0 or π . This leads to two distinct mean field states the uniform and π flux state ansatz. The uniform states ansatz is $\chi_{\vec{r},\vec{r}+\hat{x}} = \chi_{\vec{r},\vec{r}+\hat{y}} = \chi$, where $\vec{r} = (x, y)$ is the position of lattice sites. The mean field dispersion is $\epsilon(\vec{k}) = \chi[\sin(k_x) + \sin(k_y)]$ for all the three flavors, and has a square Fermi surface. However, the uniform ansatz state has higher energy than the π -flux ansatz both in mean field theory and after projection, so we focus on the π -flux ansatz.

The π -flux ansatz is $(-1)^y \chi_{\vec{r},\vec{r}+\hat{x}} = \chi_{\vec{r},\vec{r}+\hat{y}} = \chi$, as shown in FIG. 1. The unit cell in mean field theory is doubled, with u and v sublattices as shown.

After a Fourier transform, the mean field Hamiltonian

(5) is:

$$H_{\text{MF}} = (2 + \chi^2/4)L^2 + \chi \sum_{a,\vec{k}} \begin{pmatrix} c_{\alpha,\vec{k},u}^\dagger & c_{\alpha,\vec{k},v}^\dagger \end{pmatrix} \begin{pmatrix} \sin k_x & \sin k_y \\ \sin k_y & -\sin k_x \end{pmatrix} \begin{pmatrix} c_{\alpha,\vec{k},u} \\ c_{\alpha,\vec{k},v} \end{pmatrix}$$

where the sum over \vec{k} is over the $L^2/2$ (for $L \times L$ lattice) k -points in the reduced ($0 \leq k_x < 2\pi$, $0 \leq k_y < \pi$) Brillouin zone (BZ), and $a = \{1, 2, 3\}$. The above result can be further diagonalized by a Bogoliubov transformation and produce the two branches of the mean field dispersion $\epsilon_\pm(\vec{k}) = \pm\chi\sqrt{\sin^2 k_x + \sin^2 k_y}$. This dispersion has two Dirac nodes at $\vec{k} = (0, 0)$ and $(\pi, 0)$, with isotropic dispersion in their vicinity. Including flavor indices, we thus have 6 two-component Dirac fermions.

We use anti-periodic boundary conditions in both directions for $L \times L$ lattices (L even) lattices. The k -points are then $k_x = (2n + 1)\pi/L$, $n = 0 \dots L - 1$; $k_y = (2m + 1)\pi/L$, $m = 0 \dots L/2 - 1$, which avoids zero energy modes. Filling the negative energy states gives us a Slater determinant mean field wave function for each of the three fermion species. The Gutzwiller projected wave function is then easily written down as (6), in terms of this Slater determinant. Evaluating its properties however requires a numerical variational (determinantal) Monte Carlo approach.^{21,22} We generate a random initial basis state having significant overlap with the mean field wave function. Random pairs of sites are selected and updated with the Metropolis rejection rule. 10000 ‘thermalization’ sweeps (L^2 pairwise updates) are performed before measurements of physical quantities. Measurements are done in 100000 sweeps. The entire process is repeated 10 times to ensure stability of results.

Energetics: The energy from the projected wave function is listed in TABLE II for L up to 20. We notice that for the 4×4 lattice our total energy $-16.57J$ is close to the ground state energy $-17.35J$ obtained in the exact diagonalization study.³ More importantly, our energy lies below the first excited state energy $-16J$ obtained in that study, which already implies a *significant overlap* ($> 42\%$) between our wave function and the exact ground state wave function. Note, our ‘variational’ wave function has no variational parameter - which makes this agreement more remarkable, especially given that there are 24024 SU(4) singlet states already at this system size.³

We have checked several other simple states on this 4×4 lattice, they all show much higher energy, compared to the first excited state in the exact spectrum. The comparison is shown in TABLE III.

Wavefunction properties: We now provide evidence that the resulting wave function is a spin-orbital liquid. First, we would like to establish that it has no conventional order, to clearly show it is not a conventional state. Next, the specific type of liquid state being proposed - with emergent Dirac fermions and Z_2 gauge fluxes - needs to be established.

TABLE II: Results of the projected wave function on a $L \times L$ square lattice with π -flux ansatz under anti-periodic boundary conditions in both directions. The second column shows energy per site. Q_{Box} in the third column and its relation to box order is defined in main text. The fourth column shows L^{-4} scaling of spin correlation function when L is not a multiple of four [$s^z(x, y)$ is s^z at position (x, y)]. Some entries are empty because the numerical errors are too large.

L	$\langle H \rangle / L^2$	Q_{Box} / L^2	$-\langle s^z(0, 0) s^z(L/2, 0) \rangle L^4$
4	-1.0357(4)	2.0	11.14(2)
6	-0.9238(3)	1.7	20.46(5)
8	-0.9051(2)	1.7	0.0(1)
10	-0.8995(2)	1.6	20.1(2)
12	-0.8974(2)	1.6	2.7(4)
14	-0.8966(1)	1.6	18.1(4)
16	-0.8961(1)	1.6	
20	-0.8956(1)	1.6	
24	-0.8955(1)		

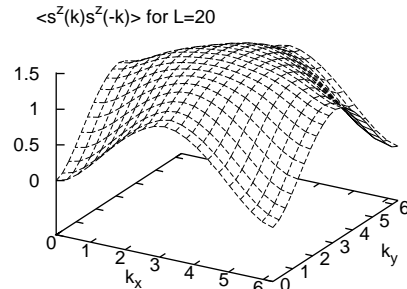
TABLE III: Energy of several (variational) states for the SU(4) model on 4×4 square lattice with periodic boundary condition.

state	energy(J)
exact ground state ³	-17.35
exact first excited state ³	-16
projected SO(6) Majorana fermion mean field	-16.57
projected SU(4) Schwinger fermion mean field	-6.38
orbital ferromagnetic, spin AFM state ^{10,23}	-14.46
box(plaquette) ordered state ¹⁰	-12
four-sublattice SU(4) Neel state ¹⁰	0

We first check for spin-orbital order. Given the SU(4) symmetry, it is sufficient to compute the s^z correlations which are found to be rapidly decaying in space. The structure factor for various lattice size was computed, e.g. FIG. 2 shows the result for the $L = 20$ lattice. A broad maximum at (π, π) is seen, but no Bragg-peak develops. We thus exclude magnetic-orbital-ordering.

A more likely order is an SU(4) singlet state that breaks lattice symmetry. This is the analog of the Valence Bond Solid order for SU(2) magnets. However, SU(4) singlets require at least four sites so box crystalline orders may arise. Two such natural orders were proposed by Li, *et al.*¹⁰ In both, the SU(4) singlets are formed on 1/4 of the elementary plaquettes, but these are either arranged in a square lattice, or in a body centered rectangular lattice with aspect ratio 2. Both box orders have bond energies modulated at the wavevectors $(\pi, 0)$ or $(\pi, \pi/2)$. We first check if our wave function has these correlations by defining $E_{x, \vec{k}} = \sum_{\vec{r}} e^{i\vec{k} \cdot \vec{r}} (s^z \tau^z)_{\vec{r}} \cdot (s^z \tau^z)_{\vec{r} + \hat{x}}$. Then $Q_{\text{Box}} = \langle E_{x, \vec{k}=(\pi, 0)}^2 \rangle$ for a $L \times L$ lattice should scale as L^4 , if long range order is present. For example, for the perfect square box state which is a product state of SU(4) singlets, $Q_{\text{Box}} = L^4/36 + (13/9)L^2$. In the absence of or-

FIG. 2: s^z structure factor for the π -flux SO(6) projected wave function on a 20×20 square lattice with anti-periodic boundary conditions.



der however, this quantity will scale as L^2 . For $L \leq 20$ we did not observe L^4 scaling but rather good L^2 scaling, as shown in Column 3 of TABLE II indicating no sign or box order upto 400 site systems. An independent check is provided by modulating the mean field parameters χ_{jk} to realize the box orders. The average energy of the projected state is then compared against the unmodulated wave function. We find that the energy always increases, for both kinds of orders, pointing to the stability of the unmodulated state. Within mean field theory alone, however, the state is locally unstable to box modulation.²⁴ The more reliable projected energy study however point to the opposite conclusion.

Motivated by a recent proposal of chiral SU(N) states in large-N limit,⁵ we also consider a chiral state on the square lattice. We add to the π -flux state pure imaginary hopping of fermions on the diagonal bonds in such a way that each triangle has $+\pi/2$ flux. This is a particular mass term of the Dirac fermions and it opens a gap in the mean field dispersion, similar to the box order mentioned above. Indeed the mean field energy decreases with the diagonal hoppings. However after projection the energy always increase after adding this term, indicating stability against this chiral order. This distinction between mean field and projected mean field energetics has been observed in other projected wave function studies as well.²⁵

We expect the spin-orbital liquid to be a nodal Z_2 state, i.e. it contains emergent Z_2 gauge fields and nodal Dirac fermions that behave like free particles at low energies. Establishing this directly is more challenging - it is well known that observing the Z_2 topological order of projected wave functions in the presence of gapless gauge charged fermions is tricky²⁶ and left to future work. Free nodal fermions would lead to spin and orbital correlations that decay as $1/r^4$, which we check for by computing $L^4 \langle s^z(0, 0) s^z(L/2, 0) \rangle$ in a size L system. The fast decay limits us to $L \leq 14$. The results are shown in column 4 of TABLE II. There are strong commensuration

FIG. 3: τ^z structure factor for the π -flux SO(6) projected wave function with average fermion filling $5/8$ for one fermion specie (other two species are still half filled), on a 20×20 square lattice with anti-periodic boundary conditions.

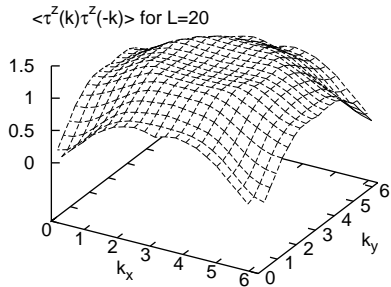
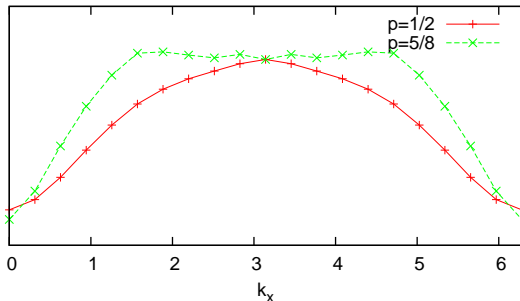


FIG. 4: (Color online) τ^z structure factor when $k_y = \pi$ (a 1D cut of FIG. 2 and FIG. 3) for the π -flux SO(6) projected wave function with average fermion filling $p = 1/2$ (green solid line with symbol +) and $p = 5/8$ (red dash line with symbol \times) for one of the three species on a 20×20 square lattice with anti-periodic boundary conditions, both curves are of arbitrary scale.



effects which reduce the correlation when $L/2$ is an even number. However, for the other three values of L the correlation seems to show the required scaling. Another indirect evidence for such fermionization is the nature of these spin correlations in the presence of a Zeeman field $\Delta H = -h \sum_r \tau_r^z$, which leads to a shifted chemical potential for one fermion specie. We find that the projected wave function now has a ring of incommensurate correlations around (π, π) (FIG. 3 and FIG. 4).

Breaking SU(4) symmetry It is natural to ask if the physical conclusions derived above are stable when enlarged SU(4) symmetry of our model is lost. Since the gauge fluxes are gapped, a weak perturbation cannot lead to confinement. Also, the gapless nodal fermions are actually protected by discrete symmetries - one needs to break lattice symmetry to gap the nodes, as can be seen from an analysis of the fermion bilinear terms (see Appendix B for details). The only physical difference that arises in the lower symmetry case is that the chemical

potential of the fermions may not be at the nodal points. Hence the SU(4) symmetry is not essential to our conclusions. In future,²⁷ we will apply this analysis to realistic Hamiltonians with reduced symmetry and search for liquid phases in those regimes.

VI. PHYSICAL REALIZATIONS

Since most natural spin orbit Hamiltonians are not near the SU(4) symmetric point, it is natural to ask where we might expect to find a model where the SU(4) symmetry is even approximately realized. As discussed in the introduction, cold atom systems in optical lattices provide some promising direction for realization, if sufficient cooling of those magnetic Hamiltonians can be achieved. In this section, we point out that even in solid state systems, approximate SU(4) symmetry may be achieved, on certain high symmetry lattices. In particular, we point out that on the *diamond* lattice, if only nearest neighbor exchange is considered, the interactions are close to the SU(4) point. Exchange interaction arises from a combination of hopping and on site interaction. The main observation is that due the high symmetry of the diamond lattice, hopping matrix elements must be SU(4) symmetric. The onsite interactions deviate from SU(4) symmetry due to, for e.g., the Hunds interaction. However, these are typically a fraction of the overall repulsion leading to nearly SU(4) symmetric exchange.

For a system of $d_{3z^2-r^2}$, $d_{x^2-y^2}$ orbitals on the diamond lattice with full lattice symmetry and without spin-orbital coupling, we first prove that the electron hopping matrix elements on nearest neighbor bonds have SU(4) symmetry. Denote the creation operators of the two orbitals as $d_{1\alpha r}^\dagger$ and $d_{2\alpha r}^\dagger$ respectively, where α is spin index, r is site index. The hopping amplitude on bond $\langle ij \rangle$ is generically a 2×2 matrix t , and the process is described by the term $\sum_{a,b,\alpha} d_{a\alpha i}^\dagger t_{ab} d_{b\alpha j}$. Consider a bond from origin along the (111) direction, the reflection $x \rightarrow y$, $y \rightarrow x$ does not change this bond, however the orbitals transform non-trivially $d_a \rightarrow \sum_b (\sigma^z)_{ab} d_b$. Since this reflection is a physical symmetry, the electronic Hamiltonian should be invariant under its action, thus we get $t = \sigma^z \cdot t \cdot \sigma^z$. Similarly consider a three-fold rotation $x \rightarrow y$, $y \rightarrow z$, $z \rightarrow x$, it does not change the (111) bond as well, but the orbitals transform as $d_a \rightarrow \sum_b [(-1/2)\sigma^z + i(\sqrt{3}/2)\sigma^y]_{ab} d_b$. Then we get $t = [(-1/2)\sigma^z - i(\sqrt{3}/2)\sigma^y] \cdot t \cdot [(-1/2)\sigma^z + i(\sqrt{3}/2)\sigma^y]$. These two conditions on t ensure that t is proportional to identity matrix. Thus we have proved that the hopping on (111) direction preserves both orbital and spin, namely is given by the term $t \sum_{a,\alpha} d_{a\alpha i}^\dagger d_{a\alpha j}$. By lattice symmetry we conclude that all other nearest neighbor hoppings have this property. Therefore the nearest neighbor hoppings have SU(4) symmetry. One should note that this proof cannot be extended to next nearest neighbor and other generic hoppings.

However, the Coulomb interaction of these orbitals generically does not have SU(4) symmetry. The onsite Coulomb interaction is given by the Kanamori parameters,²⁸ $U \sum_a n_{a\uparrow} n_{a\downarrow} + U' \sum_{a<b} n_a n_b + J \sum_{a<b,\alpha,\beta} d_{a\alpha}^\dagger d_{b\beta}^\dagger d_{a\beta} d_{b\alpha} + J \sum_{a<b} (d_{a\uparrow}^\dagger d_{a\downarrow}^\dagger d_{b\downarrow} d_{b\uparrow} + \text{h.c.})$, and approximately $U = U' + 2J$. The SU(4) symmetry is present only if $J = 0$ and $U = U'$. We usually expect that $J \ll U$, then SU(4) is an approximate symmetry of the Hubbard model and thus an approximate symmetry of the derived spin-orbital exchange model.

This type of systems may be realized in certain A-site spinels, where the magnetic ions form a diamond lattice, and when only the e_g orbitals are active. One caveat is that the spinel structure allows for the next nearest neighbor exchange strength to be fairly large and even comparable to the nearest neighbor one, which may significantly break the SU(4) symmetry. Interestingly, the experimentally discussed ‘spin-orbital’ liquid candidate, FeSc₂S₄, is an e_g system on the diamond lattice.⁴ However, it differs in two important respects from the ideal model considered here. First, there is a magnetic moment on each site that is Hunds coupled to the e_g fermion, and second, the further neighbor exchange interactions are believed to be substantial in this material.

We acknowledge support from nsf-dmr0645691, and discussions with M. Hermele.

APPENDIX A: PROOF OF THE EQUIVALENCE BETWEEN PROJECTED SO(6) MAJORANA MEAN FIELD STATE AND PROJECTED SU(4) SCHWINGER FERMION MEAN FIELD STATE FOR 1D CHAIN.

Consider a $4N$ -site chain with periodic boundary condition. The mean field wave function for the Majorana fermion representation is

$$|\Psi_{\text{MF}}\rangle = \prod_{k=0}^{2N-1} \tilde{c}_{1,(2k+1)\pi/(4N)}^\dagger \prod_{k=0}^{2N-1} \tilde{c}_{2,(2k+1)\pi/(4N)}^\dagger \times \prod_{k=0}^{2N-1} \tilde{c}_{3,(2k+1)\pi/(4N)}^\dagger |0\rangle \quad (\text{A1})$$

where $|0\rangle$ is fermion vacuum, $\tilde{c}_{\alpha,k}$ is the Fourier transform of real space fermion operator $\tilde{c}_{\alpha,k} = (4N)^{-1/2} \sum_r c_{\alpha,r} e^{-ikr}$. For a physically allowed real space configuration mentioned above $|\{x_i\}, \{y_j\}, \{z_m\}\rangle = \prod_{i=1}^N (c_{2x_i}^\dagger c_{3x_i}^\dagger) \prod_{j=1}^N (c_{3y_j}^\dagger c_{1y_j}^\dagger) \prod_{m=1}^N (c_{1z_m}^\dagger c_{2z_m}^\dagger) |0\rangle$, the overlap with the mean field wave function is

$$\Psi[\{x_i\}, \{y_j\}, \{z_m\}] = \langle \{x_i\}, \{y_j\}, \{z_m\} | \Psi_{\text{MF}} \rangle = \Phi[\{y_j\}, \{z_m\}] \cdot \Phi[\{z_m\}, \{x_i\}] \cdot \Phi[\{x_i\}, \{y_j\}] \quad (\text{A2})$$

where Φ is the $2N \times 2N$ Slater determinant for one fermion specie with the following matrix elements ($p, q =$

$1, \dots, 2N$)

$$\sqrt{4N} \cdot \Phi[\{x_i\}, \{y_j\}]_{pq} = \begin{cases} e^{\frac{i\pi(2p-1)x_q}{4N}}, & q \leq N; \\ e^{\frac{i\pi(2p-1)y_{q-N}}{4N}}, & N < q. \end{cases} \quad (\text{A3})$$

Therefore the determinant is

$$\begin{aligned} & \Phi[\{x_i\}, \{y_j\}] \\ &= (4N)^{-N} \omega^{(\sum_i x_i + \sum_j y_j)} \prod_{i,j} (\omega^{2y_j} - \omega^{2x_i}) \\ & \times \prod_{i>i'} (\omega^{2x_i} - \omega^{2x_{i'}}) \prod_{j>j'} (\omega^{2y_j} - \omega^{2y_{j'}}) \end{aligned} \quad (\text{A4})$$

where $\omega = e^{i\pi/(4N)}$. And the overlap is

$$\begin{aligned} & \Psi[\{x_i\}, \{y_j\}, \{z_m\}] \\ &= (4N)^{-3N} \omega^{2 \cdot (\sum_i x_i + \sum_j y_j + \sum_m z_m)} \\ & \times \prod_{i,j} (\omega^{2y_j} - \omega^{2x_i}) \prod_{j,m} (\omega^{2z_m} - \omega^{2y_j}) \\ & \times \prod_{m,i} (\omega^{2x_i} - \omega^{2z_m}) \prod_{i>i'} (\omega^{2x_i} - \omega^{2x_{i'}})^2 \\ & \times \prod_{j>j'} (\omega^{2y_j} - \omega^{2y_{j'}})^2 \prod_{m>m'} (\omega^{2z_m} - \omega^{2z_{m'}})^2 \end{aligned} \quad (\text{A5})$$

The mean field Hamiltonian for the standard ‘Schwinger’ fermion representation is

$$\begin{aligned} H_{\text{MF},a} &= \chi \sum_r \sum_{\alpha=1}^4 a_{\alpha,r}^\dagger a_{\alpha,r+1} + \text{h.c.} - \mu \sum_r \sum_{\alpha=1}^4 a_{\alpha,r}^\dagger a_{\alpha,r} \\ &= \chi \sum_r \sum_{\alpha=1}^3 a_{\alpha,r}^\dagger a_{\alpha,r+1} - \chi \sum_r a'_{4,r}^\dagger a'_{4,r+1} + \text{h.c.} \\ & \quad - \mu \sum_r \sum_{\alpha=1}^3 a_{\alpha,r}^\dagger a_{\alpha,r} + \mu \sum_r a'_{4,r}^\dagger a'_{4,r} \end{aligned} \quad (\text{A6})$$

where a' is the particle-hole conjugate of the Schwinger fermion a . The particle-hole transformation on the fourth specie is required for the following projected wave function to represent a bosonic spin-orbital wave function. The quarter-filling mean field wave function for the standard fermionic representation is (we assume N is even for simplicity)

$$\begin{aligned} & |\Psi_{\text{MF}}\rangle_a \\ &= \prod_{k=-N/2}^{N/2-1} \tilde{a}_{1,(2k+1)\pi/(4N)}^\dagger \prod_{k=-N/2}^{N/2-1} \tilde{a}_{2,(2k+1)\pi/(4N)}^\dagger \\ & \times \prod_{k=-N/2}^{N/2-1} \tilde{a}_{3,(2k+1)\pi/(4N)}^\dagger \prod_{k=-7N/2}^{-N/2-1} \tilde{a}'_{4,(2k+1)\pi/(4N)}^\dagger |0'\rangle \end{aligned} \quad (\text{A7})$$

where $\tilde{a}_{\sigma,k}$ is the Fourier transform of the real space SU(4) ‘Schwinger fermions’ $\tilde{a}_{\sigma,k} = (4N)^{-1/2} e^{-ikr} a_{\sigma,r}$,

and $|0'\rangle$ is the fermion ‘vacuum’ that can be annihilated by a_1, a_2, a_3 and the particle-hole conjugate of the fourth specie a_4^\dagger .

A physically allowed real space configuration in this representation is still labeled by three sets of N distinct numbers $\{x_i\}, \{y_j\}, \{z_m\}$,

$$\begin{aligned} |\{x_i\}, \{y_j\}, \{z_m\}\rangle &= \prod_{i=1}^N a_{1,x_i}^\dagger \prod_{j=1}^N a_{2,y_j}^\dagger \prod_{m=1}^N a_{3,z_m}^\dagger \\ &\quad \times \prod_{i=1}^N a_{4,x_i}^\dagger \prod_{j=1}^N a_{4,y_j}^\dagger \prod_{m=1}^N a_{4,z_m}^\dagger |0'\rangle \end{aligned} \quad (\text{A8})$$

The overlap of this configuration with the mean field wave function is the product of four Slater determinants,

$$\begin{aligned} \Psi_a[\{x_i\}, \{y_j\}, \{z_m\}] &= \langle \{x_i\}, \{y_j\}, \{z_m\} | \Psi_{\text{MF}} \rangle_a \\ &= \Phi_a[\{x_i\}] \cdot \Phi_a[\{y_j\}] \cdot \Phi_a[\{z_m\}] \cdot \Phi_{a'}[\{x_i\}, \{y_j\}, \{z_m\}] \end{aligned} \quad (\text{A9})$$

The $N \times N$ Slater determinants Φ_a has the following matrix elements ($p, q = 1, \dots, N$), $\Phi_a[\{x_i\}]_{pq} = (4N)^{-1/2} e^{\frac{i\pi(2p-1-N)x_q}{4N}}$. The matrix elements of the $3N \times 3N$ Slater determinant $\Phi_{a'}$ is ($p, q = 1, \dots, 3N$)

$$\begin{aligned} \Phi_{a'}[\{x_i\}, \{y_j\}, \{z_m\}]_{pq} &= \begin{cases} e^{\frac{i\pi(2p-1-7N)x_q}{4N}}, & q \leq N \\ e^{\frac{i\pi(2p-1-7N)y_{q-N}}{4N}}, & N < q \leq 2N \\ e^{\frac{i\pi(2p-1-7N)z_{q-2N}}{4N}}, & 2N < q \leq 3N \end{cases} \end{aligned} \quad (\text{A10})$$

Therefore the determinant of Φ_a is

$$\Phi_a[\{x_i\}] = (4N)^{-N/2} \omega^{(1-N) \cdot (\sum_i x_i)} \prod_{i>i'} (\omega^{2x_i} - \omega^{2x_{i'}}) \quad (\text{A11})$$

And the determinant of $\Phi_{a'}$ is

$$\begin{aligned} \Phi_{a'}[\{x_i\}, \{y_j\}, \{z_m\}] &= (4N)^{-3N/2} \omega^{(1-7N) \cdot (\sum_i x_i + \sum_j y_j + \sum_m z_m)} \\ &\quad \times \prod_{i,j} (\omega^{2y_j} - \omega^{2x_i}) \prod_{j,m} (\omega^{2z_m} - \omega^{2y_j}) \\ &\quad \times \prod_{m,i} (\omega^{2z_m} - \omega^{2x_i}) \prod_{i>i'} (\omega^{2x_i} - \omega^{2x_{i'}}) \\ &\quad \times \prod_{j>j'} (\omega^{2y_j} - \omega^{2y_{j'}}) \prod_{m>m'} (\omega^{2z_m} - \omega^{2z_{m'}}) \end{aligned} \quad (\text{A12})$$

Finally the overlap between this basis state and the mean

field wave function is (note that $\omega^{8N} = 1$)

$$\begin{aligned} \Psi_a[\{x_i\}, \{y_j\}, \{z_m\}] &= (4N)^{-3N} (-1)^{N^2} \omega^{(2-8N) \cdot (\sum_i x_i + \sum_j y_j + \sum_m z_m)} \\ &\quad \times \prod_{i,j} (\omega^{2y_j} - \omega^{2x_i}) \prod_{j,m} (\omega^{2z_m} - \omega^{2y_j}) \\ &\quad \times \prod_{m,i} (\omega^{2x_i} - \omega^{2z_m}) \prod_{i>i'} (\omega^{2x_i} - \omega^{2x_{i'}})^2 \\ &\quad \times \prod_{j>j'} (\omega^{2y_j} - \omega^{2y_{j'}})^2 \prod_{m>m'} (\omega^{2z_m} - \omega^{2z_{m'}})^2 \\ &= (-1)^{N^2} \omega^{-8N(\sum_i x_i + \sum_j y_j + \sum_m z_m)} \Psi[\{x_i\}, \{y_j\}, \{z_m\}] \\ &= (-1)^{N^2} \Psi[\{x_i\}, \{y_j\}, \{z_m\}] \end{aligned} \quad (\text{A13})$$

Therefore these two projected wave functions for 1D chain are identical. The crucial property utilized was that the Slater determinants appearing are Vandermonde determinants in one dimension. This property does not hold in higher dimensions.

APPENDIX B: PROJECTIVE SYMMETRY GROUP ANALYSIS OF FERMION BILINEARS IN THE π -FLUX STATE ON SQUARE LATTICE

For the π -flux ansatz in FIG. 1 on an infinite lattice the lattice group symmetries are realized as follows (flavor index α omitted):

$$\begin{aligned} T_x &: c_{(x,y)} \rightarrow c_{(x+1,y)} \\ T_y &: c_{(x,y)} \rightarrow (-1)^x c_{(x,y+1)} \\ R_{\pi/2} &: c_{(x,y)} \rightarrow \frac{1 + (-1)^y - (-1)^x + (-1)^{x+y}}{2} c_{(-y,x)} \\ m_y &: c_{(x,y)} \rightarrow (-1)^x c_{(-x,y)} \end{aligned}$$

Define a 4-component field

$$\psi_{\alpha, \vec{k}} = [c_{\alpha, \vec{k}, u}, c_{\alpha, \vec{k}, v}, c_{\alpha, (\pi, 0) + \vec{k}, v}, c_{\alpha, (\pi, 0) + \vec{k}, u}]$$

linearize the dispersion around the Dirac point, the low-energy Hamiltonian becomes

$$\chi \sum_{\alpha, |\vec{k}| \ll 1} \psi_{\alpha, \vec{k}}^\dagger [k_x \mathbb{1} \otimes \mu^z + k_y \mathbb{1} \otimes \mu^x] \psi_{\alpha, \vec{k}}$$

where μ are Pauli matrices acting on the u, v 2D space. The original fermion in real space can be represented as $c_{\alpha, \vec{r}} = N_{\text{site}}^{-1/2} \sum_{|\vec{k}| \ll 1} e^{i\vec{k} \cdot \vec{r}} \{ [1 + (-1)^y] \cdot [(\psi_{\alpha, \vec{k}})_1 + (-1)^x (\psi_{\alpha, \vec{k}})_4] + [1 - (-1)^y] \cdot [(\psi_{\alpha, \vec{k}})_2 + (-1)^x (\psi_{\alpha, \vec{k}})_3] \} / 2$ where $\vec{r} = (x, y)$. Then we have the transformation property of the ψ field

$$\begin{aligned} T_x &: \psi_{(k_x, k_y)} \rightarrow \nu^z \otimes \mathbb{1} \psi_{(k_x, k_y)} \\ T_y &: \psi_{(k_x, k_y)} \rightarrow \nu^x \otimes \mathbb{1} \psi_{(k_x, k_y)} \\ R_{\pi/2} &: \psi_{(k_x, k_y)} \rightarrow (1/2)(1 + i\nu^y) \otimes (1 + i\mu^y) \psi_{(-k_y, k_x)} \\ m_y &: \psi_{(k_x, k_y)} \rightarrow \nu^x \otimes \mu^x \psi_{(-k_x, k_y)} \end{aligned}$$

where $\nu^{x,y,z}$ are Pauli matrices acting on the 2D space of the two Dirac nodes $(0,0)$ and $(\pi,0)$. The low energy Hamiltonian is invariant under these transformations. In the following we will prove that these symmetries prohibit mass term and velocity anisotropy in the low energy theory.

Consider a general mass term $\psi^\dagger M \psi$ where M is a 4×4 constant non-trivial (not proportional to identity) Hermitian matrix. T_x and T_y translation symmetries require that $M \propto \mathbb{1} \otimes \mu$ with μ be a 2×2 constant Hermitian matrix. m_y reflection symmetry requires $\mu \propto \mu^x$, but this violate the $R_{\pi/2}$ rotation symmetry and is forbidden.

Consider a general velocity anisotropy term $\psi^\dagger (k_x M_1 + k_y M_2) \psi$ with constant 4×4 matrices M_1 and M_2 . Again T_x and T_y translation symmetries require that $M_{1(2)} \propto \mathbb{1} \otimes \mu_{1(2)}$. m_y reflection symmetry requires $\mu^x \mu_1 \mu^x = -\mu_1$ and $\mu^x \mu_2 \mu^x = \mu_2$, therefore $\mu_2 \propto \mu^x$. Also consider 180° rotation $R_{\pi/2}^2$ symmetry $\psi_{(k_x, k_y)} \rightarrow -\nu^y \otimes \mu^y \psi_{(-k_x, -k_y)}$, it requires $\mu^y \mu_1 \mu^y = -\mu_1$, thus $\mu_1 \propto \mu^z$. Now we have $\psi^\dagger (A k_x \mathbb{1} \otimes \mu^z + B k_y \mathbb{1} \otimes \mu^x) \psi$ with constants A, B . Use the 90° rotation symmetry $R_{\pi/2}$ we get

$$\begin{aligned} & A(-k_y) \mathbb{1} \otimes \mu^z + B k_x \mathbb{1} \otimes \mu^x \\ &= A k_x \mathbb{1} \otimes [(1 - i\mu^y) \mu^z (1 + i\mu^y)]/2 \\ & \quad + B k_y \mathbb{1} \otimes [(1 - i\mu^y) \mu^x (1 + i\mu^y)]/2 \\ &= A k_x \mathbb{1} \otimes \mu^x - B k_y \mathbb{1} \otimes \mu^z \end{aligned}$$

Then we have $B = A$ and this term is just the kinetic

energy term in the Hamiltonian.

Consider a general bilinear term $\psi^\dagger M(k_x, k_y) \psi$ where $M(k_x, k_y)$ is a 4×4 hermitian matrix and a homogeneous polynomial of k_x, k_y . From translation symmetries it must be of the form $\mathbb{1} \otimes [m_0(k_x, k_y) \mathbb{1} + m_1(k_x, k_y) \mu^x + m_2(k_x, k_y) \mu^y + m_3(k_x, k_y) \mu^z]$ where $m_{0,1,2,3}$ are homogeneous functions of k_x, k_y and are of the same order. From m_y reflection symmetry,

$$\begin{aligned} m_0(-k_x, k_y) &= m_0(k_x, k_y), \\ m_1(-k_x, k_y) &= m_1(k_x, k_y), \\ m_2(-k_x, k_y) &= -m_2(k_x, k_y), \\ m_3(-k_x, k_y) &= -m_3(k_x, k_y) \end{aligned}$$

From $R_{\pi/2}$ rotation symmetry,

$$\begin{aligned} m_0(-k_y, k_x) &= m_0(k_x, k_y), \\ m_3(-k_y, k_x) &= -m_1(k_x, k_y), \\ m_2(-k_y, k_x) &= m_2(k_x, k_y), \\ m_1(-k_x, k_y) &= m_3(k_x, k_y) \end{aligned}$$

This requires that m_0 is of the form $\tilde{m}_0(k_x^2 + k_y^2, k_x^2 k_y^2)$, m_1 is $k_y \tilde{m}_1(k_x^2, k_y^2)$, m_2 is $k_x k_y (k_x^2 - k_y^2) \tilde{m}_2(k_x^2 + k_y^2, k_x^2 k_y^2)$, and m_3 is $k_x \tilde{m}_3(k_y^2, k_x^2)$, where $\tilde{m}_0, \tilde{m}_1, \tilde{m}_2$ are arbitrary polynomials.

-
- ¹ L. F. Feiner, A. M. Oles, and J. Zaanen, Phys. Rev. Lett. **78**, 2799 (1997).
² G. Khaliullin and S. Maekawa Phys. Rev. Lett. **85**, 3950 (2000)
³ Mathias van den Bossche, F.-C. Zhang, F. Mila, Euro. Phys. J. B **17**, 367 (2000).
⁴ V. Fritsch, *et al.*, Phys. Rev. Lett. **92**, 116401 (2004).
⁵ M. Hermele, V. Gurarie, A. M. Rey, arXiv:0906.3718
⁶ T. Fukuhara, Yosuke Takasu, Mitsutaka Kumakura, and Yoshiro Takahashi, Phys. Rev. Lett. **98**, 030401 (2007).
⁷ T. Fukuhara, Seiji Sugawa, Masahito Sugimoto, Shintaro Taie, and Yoshiro Takahashi, Phys. Rev. A **79**, 041604(R) (2009).
⁸ Congjun Wu, Mod. Phys. Lett. B **20**, 1707 (2006).
⁹ K. I. Kugel, and D. I. Khomskii, Sov. Phys. Usp. **25**, 231 (1982).
¹⁰ Y. Q. Li, Michael Ma, D. N. Shi, F. C. Zhang, Phys. Rev. Lett. **81**, 3527 (1998).
¹¹ P. W. Anderson, Mater. Res. Bull. **8**, 153 (1973).
¹² D. S. Rokhsar, and S. A. Kivelson, Phys. Rev. Lett. **61**, 2376 (1988).
¹³ S.-Q. Shen, G.-M. Zhang, Europhys. Lett. **57**, 274 (2002).
¹⁴ A. Mishra, M. Ma, and F.-C. Zhang, Phys. Rev. B **65**, 214411 (2002).
¹⁵ A. Tsvelik, Quantum Field Theory in Condensed Matter Physics, Cambridge University Press (1995).
¹⁶ A. Kitaev, Annals of Physics **321**, 2 (2006).
¹⁷ B. Sutherland, Phys. Rev. B **12**, 3795 (1975).
¹⁸ P. Azaria, A. O. Gogolin, P. Lecheminant, A. A. Nersisyan, Phys. Rev. Lett. **83**, 624 (1999).
¹⁹ I. Affleck, Nucl. Phys. B **265**, 409 (1986).
²⁰ S. K. Pati, R. R. P. Singh, and D. I. Khomskii, Phys. Rev. Lett. **81**, 5406 (1998).
²¹ C. Gros, Annals of Physics **189**, 53 (1989).
²² D. Ceperley, G. V. Chester, and M. H. Kalos, Phys. Rev. B **16**, 3081 (1977).
²³ M. Gross, E. Sanchez-Velasco, and Eric Siggia Phys. Rev. B **39**, 2484 (1989)
²⁴ I. Affleck, and J. B. Marston, Phys. Rev. B **37**, 3774 (1988).
²⁵ Y. Ran, M. Hermele, P. A. Lee, X.-G. Wen, Phys. Rev. Lett. **98**, 117205 (2007)
²⁶ D. A. Ivanov, T. Senthil, Phys. Rev. B **66**, 115111 (2002).
²⁷ Fa Wang and Ashvin Vishwanath, in progress.
²⁸ C. Castellani, C. R. Natoli, J. Ranninger, Phys. Rev. B **18**, 4945 (1978); R. Fresard, G. Kotliar, Phys. Rev. B **56**, 12909 (1997).